Research on Chemical Intermediates
https://doi.org/10.1007/s11164-023-05158-5

ORIGINAL ARTICLE

Utilisation of coal tar naphthalene oil fractions for the synthesis of value-added chemicals: alternative paths to mono- and di-methylnaphthalenes

Fatih Güleç[1,2] · Aysun Koçkan[3] · Ali Karaduman[3]

Received: 23 July 2023 / Accepted: 27 September 2023
© The Author(s) 2023

Abstract

This study investigates the utilisation of coal tar naphthalene oil fraction (CTNOF), an economical by-product derived from the iron-steel industry, for the production of valuable chemicals, with a particular focus on methylnaphthalenes (MNs) and dimethylnaphthalenes (DMNs). Of specific interest is 2,6-dimethylnaphthalene (2,6-DMN), a pivotal component in the manufacture of polyethylene naphthalate (PEN). The intricate and costly nature of 2,6-DMN production currently poses challenges to the commercial viability of PEN. This study provides the potential heterogeneous reaction pathways for the synthesis of MNs and DMNs via methylation, disproportionation, and isomerisation of CTNOF. The utilisation of CTNOF was investigated in a laboratory-scale fixed bed reactor operating at atmospheric pressure using a mixture of CTNOF: methanol having 1:5 mass ratio over HBeta zeolite catalyst at a temperature of 400 °C and weight hourly space velocity of 2 h^{-1}. The results reveal the successful methylation of CTNOF over the HBeta zeolite catalyst, initially achieving high naphthalene conversion, particularly into 2-MN. This highlights the potential of CTNOF as an alternative feedstock for the production of value-added chemicals. While naphthalene conversion initially reaches 99 wt% within 0.5 h of operation, it gradually decreases to approximately 10 wt% over extended run times. Notably, coke deposition significantly deactivates the HBeta zeolite catalyst during CTNOF methylation, impacting naphthalene conversion. A substantial proportion of naphthalene compounds convert to methylnaphthalenes early in the reaction, predominantly 2-MN, increasing from 14 wt% (in CTNOF feedstock) to 87 wt%. Among DMNs, selectivity for 2,6-DMN, 2,7-DMN, 1,3-DMN, and 1,7-DMN increases, while other DMN isomers exhibit a sharp decrease in selectivity. The distribution of 2,6-triad DMNs rises from 38 wt% in feedstocks to 52–55 wt% with extended reaction times, attributed to MN conversion to DMNs and potential isomerisation from other DMNs. This study underscores the feasibility of using CTNOF for the direct synthesis of valuable chemicals, specifically 2,6-DMN and 2-MN, through methylation over HBeta zeolite catalysts. However, it emphasises the

Extended author information available on the last page of the article

Published online: 15 October 2023

critical role of residence time in coke deposition and the need for optimisation, particularly regarding this parameter, to ensure the efficiency of this catalytic process.

Keywords Naphthalene · Methylnaphthalene · Dimethylnaphthalene · Value-added chemicals · Methylation · Zeolite catalysts

Introduction

Coal tar naphthalene oil fraction (CTNOF) is typically obtained as a by-product of the coking process in steel production. When coal is subjected to high temperatures in the absence of air (coking), it undergoes thermal decomposition, yielding various by-products including coal tar [1]. This tar can be further processed to extract different fractions, one of which is naphthalene oil [2, 3]. In an average-sized iron-steel facility, the production of coal tar can range from hundreds to thousands of tons per day. Iron-steel industries therefore tend to facilitate coal tar deep processing projects, i.e., Wuhan Iron and Steel (Group) Company—1 million t/a of coal tar deep processing project started [4]. As the naphthalene oil fraction can account for around 9–12% of the total weight of the tar and contains naphthalene, phenol, cresols, xylenols, and heavy pyridine base [4]. Therefore, in a facility producing, for example, 1000 tons of coal tar per day, the naphthalene oil fraction could potentially be around 90–120 tons daily (it is important to note that these figures are approximate and can differ based on the specific processes and technologies employed by each steel facility. Additionally, production levels can be influenced by market demands and environmental regulations that might impact the amount of coal tar derived and processed for naphthalene oil). The market for coal tar naphthalene oil is diverse and encompasses various sectors due to its wide range of applications [4, 5]. Naphthalene is utilised in the textile sector for dyeing and finishing processes [6]. It plays a crucial role in the creation of azo dyes, surfactants, and dispersants, offering its versatility to multiple sectors, including textiles[6], construction, and chemicals[7–9]. Coal tar naphthalene oil can also be employed in the manufacturing of rubber and plastic products [4, 10, 11] used in the automotive sector. Naphthalene compounds derived from coal tar can be used in the production of synthetic pharmaceutical compounds [12, 13] and synthetic chemicals as methylnaphthalenes, dimethylnaphthalenes [8, 9, 14–16].

As CTNOF consists mainly of naphthalene fractions, it can be used to produce methylnaphalenes (MNs; 1-MN and 2-MN) and dimethylnaphalenes (DMNs; 2,7-DMN, 2,6-DMN, 2,3-DMN, 1,8-DMN, 1,7-DMN, 1,6-DMN, 1,5-DMN, 1,4-DMN, 1,3-DMN, 1,2-DMN). Among these products, 2-methylnaphthalene (2-MN) and 2,6-dimethylnaphthalene (2,6-DMN) are the most important two organic compounds. 2-MN is used for the production of vitamin K [17, 18] and 2,6-DMN [19–24]. 2,6-DMN is a vital component for the synthesis of advanced polyester resins, including polyethylene naphthalate (PEN) and polybutylene naphthalate (PBN). PEN has exceptional properties such as an improved barrier to gases, greater tensile strength, better resistance to heat, and stability against UV light and X-rays

compared to polyethylene terephthalate (PET) [25]. As a result, there is significant potential for PEN to be used in various applications such as in films and bottles, refillable containers, advanced photography systems, and tire codes. The intended uses for PBN include electronics, insulation, and automotive parts [26]. However, the complex synthesis process and the absence of a reliable and efficient method for producing 2,6-dimethylnaphthalene commercially have limited the practical application of both PEN and PBN in the industry [24, 26].

In order to produce 2,6-DMN, a few synthesis procedures have been proposed; the first one is the synthesis of 2,6-DMN with methylation, disproportionation, and trans-alkylation of naphthalene sources such as 2-MN [19, 20, 22, 27–32] and naphthalene [25, 33–35], the second one is isomerisation of MNs [36] DMNs [26, 36, 37]. Although studies have been using pure naphthalene or 2-MN as a feedstock in these reactions, the conversion of naphthalene or 2-MN and the selectivity of 2,6-DMN is relatively low. The rich naphthalene fraction contents (naphthalene, MNs, and DMNs) make CTNOF an alternative and cost-effective feedstock for the synthesis of 2-MN and 2,6-DMNs through methylation, disproportionation, and isomerisation reactions. Although CTNOF has been used for the synthesis of value-added chemicals via hydrotreatment [38], purification of naphthalene [39], separation of the phenolic compounds by liquid–liquid extraction [40], and the extraction and fractionation of supercritical fluid from high-temperature coal tar [41], there is no investigation on direct synthesis of value-added chemicals (2-MN and 2,6-DMN) via methylation, isomerisation, and disproportionation.

The direct production of 2,6-dimethylnaphthalene has been studied through the methylation and disproportionation of a naphthalene source using various types of zeolite catalysts. Wu et al. [42] explored the impact of Al, Ga and Al–Ga impregnated ZSM-12 on the methylation of naphthalene. Song et al. [30] examined the selective methylation of naphthalene to produce 2,6-DMN using Ti, Co, and Fe modified ZSM-5 zeolite catalysts. The Fe modification improved the conversion, selectivity towards 2,6-DMN, and the 2,6-DMN/2,7-DMN ratio. Motoyuki et al. [26] studied the isomerisation of DMNs to produce 2,6-DMN using a non-valuable feed stream that primarily consisted of naphthalene and DMN isomers [26]. The methylation of 2-MN was also investigated using various zeolites such as Pt, Fe, Ti, Zr and Co-doped ZSM-5 and La, Cu-doped Y zeolite by Jin et al. [22], Zhao et al. [43], Pu and Inui [25], and Niftaliyeva et al. [44, 45]. Higher ratios of 2,6-DMN/2,7-DMN, increased selectivity towards 2,6-DMN, and higher yields of 2,6-DMN were obtained over Zr/ZSM-5 [22]. Zhao et al. [43] found that the Pt modified ZSM-5 catalyst showed lower coke formation and greater conversion of 2-MN, higher selectivity, and higher yield of 2,6-DMN compared to HZSM-5.

Although there are few studies about the synthesis of 2,6-DMN, an economical process and desired values have not been developed yet. Using a non-valuable feed stream, which mainly consists of naphthalene sources, in the production procedure may, therefore, significantly decrease the production costs. CTNOF has a good potential as a feedstock for the synthesis of 2-MN and 2,6-DMN. In this study, CTNOF was, therefore, investigated as the feedstock of synthesis of value-added chemicals such as 2-MN and 2,6-DMN. The aim of this study is to investigate methylation and isomerisation of CTNOF on HBeta zeolite catalyst and enriched

the 2-MN and 2,6-DMN content of CTNOF effectively. To reach high 2-MN and 2,6-DMN selectivity, Beta zeolite catalyst were used as it can be used as both methylation [23, 33] and isomerisation [46–48] catalyst, which potentially provide higher selectivity values in these types of feed streams.

Materials and experimental method

Catalyst preparation and characterisation

In order to synthesise hydrogen form beta zeolite, we sourced ammonium form beta (NH_4-beta) zeolite catalysts from ACS Material Corporation. The conversion of NH_4-beta zeolite to its hydrogen form involved an activation process, where ammonium ions were replaced with hydrogen ions. This activation was achieved by gradually heating the NH_4-beta zeolite under controlled heating conditions in a dry airflow atmosphere. Approximately 10 g of NH_4-beta zeolite were placed in a porcelain crucible and subjected to the following temperature procedure: heating from room temperature to 350 °C over 30 min, followed by a 3-h hold at 350 °C. Subsequently, the catalysts were heated from 350 to 850 °C at a rate of 20 °C/min and maintained at the target temperature for 4 h. The resulting catalyst was designated as the hydrogen form beta catalyst (HBeta). Detailed physical and chemical properties of the HBeta zeolite are outlined in Table 1.

XRD analysis the crystalline phases of HBeta was measured using an Inel Equinox 1000 X-ray powder diffractometer (XRD) with Cu-Kα operating at 40 kV and 35 mA. The catalyst was scanned over a $2\theta = 5°–70°$ with 0.05° as step size and 2 s as step time. *SEM and EDS analysis* the surface morphology of the catalysts was scanned at the magnifications of 2 µm at 20 kV accelerated voltage using secondary electron imaging (SEI) modes by SEM (ZEISS EVO 40). Additionally, the elemental characterisation has been identified by energy-dispersive X-ray spectroscopy (EDX) mapping and spectrums using Oxford X-Max spectroscopy. N_2

Table 1 Physical and chemical properties of HBeta zeolite catalyst

Properties	Unit	Value
Average pore size	nm	0.6–0.8
Particle shape	–	Granular (*D*: 6–8 mm)
Cristal size	mm	100–200
Cation form	–	H^+
BET surface area	m^2/g	432
BJH pore diameter	Å	34.09
BJH pore volume	cm^3/g	0.345
Silica (Si)	%	40.3
Alumina (Al)	%	7.40
Oxygen (O)	%	52.3

adsorption–desorption analysis the textural properties of the HBeta were measured by nitrogen sorption were conducted using a Quantachrome NOVA 2200 series volumetric gas adsorption instrument. Prior to analysis, in order to remove moisture and adsorbed gases, the ~1.0 g of HBeta catalyst was degassed at 150 °C for 15 h under vacuum conditions. The nitrogen isotherms have measured a range of relative pressures (P/P°) from 0.01 to 0.99 at − 196 °C in liquid nitrogen. The specific surface area of the catalyst was calculated according to the Brunauer, Emmett, and Teller (BET) method, and the pore volume was determined using Barrett, Joyner, and Halenda (BJH) method using Microactive Software V3.0. *XRF analysis* the quantity of metal forms of HBeta catalyst was measured by X-ray fluorescence (XRF) using Spectra XLAB2000 PEDX-ray fluorescence. The samples having a powder form were filled in a pot having a diameter of 27 mm. A thin Prolene film having a thickness of 4.0 µm placed at the bottom of the pot, allowed for the X-rays to quantitatively measure the elemental composition of the samples using a 40-kV Ag-anode X-ray tube, calibrated by internal Omnion calibration programme. *Acidity of catalysts* in order to identify the Brønsted and Lewis acid sites present in HBeta, infrared analyses were carried out using a Mattson 1000 FTIR spectrometer.

Composition of coal tar naphthalene oil fraction

The coal tar naphthalene oil fraction (CTNOF) was supplied from Kardemir Iron-Steel Industry (Turkey). The chemical compositions of CTNOF was identified and characterised using the following procedure. Approximately 5.0 g of CTNOF was diluted in 50 ml of Tetrahydrofuran (THF, C_4H_8O, bp: 66 °C) and analysed in a gas chromatography (Thermo Finnigan DSQ 250) having a 60 m × 0.25 mm × 0.25 µm capillary column and characterised by a Mass Spectroscopy (MS, Zebron, ZB-1 ms). An aliquot, 1 µl, of the sample (diluted in THF) was injected at 250 °C with helium as the carrier gas. The oven temperature was programmed from 95 to 125 °C at a heating rate of 1 °C/min, 125–200 °C at a heating rate of 5 °C, and finally, 200–230 °C at a heating rate of 20 °C/min.

Methylation of coal tar naphthalene oil fraction

Tests to methylate the coal tar naphthalene oil fraction (CTNOF) were performed using a setup that consisted of a high-pressure liquid pump, a flow meter in a fixed-bed flow reactor surrounded by a furnace with a temperature control system, a condenser, a phase separator, and a gas chromatography–mass spectrometer (GC–MS). This setup was described in Fig. 1 of references [24, 44]. The feed stream was prepared using a mixture of CTNOF and methanol having 1:5 mass ratio. Approximately 1 g (2 ml) of HBeta zeolite catalyst was located in the centre of the fixed-bed reactor, the catalysts were activated under N_2 atmosphere (5 ml/min) at 500 °C for 30 min. When the temperature decreased to the reaction temperature (400 °C), the reaction mixture (CTNOF: methanol) was introduced to the fixed-bed reactor at atmospheric pressure by a high-pressure liquid pump at a weight hourly space velocity of 2 h^{-1}. The reaction products were cooled down to − 10 °C and the product collection was based on the time

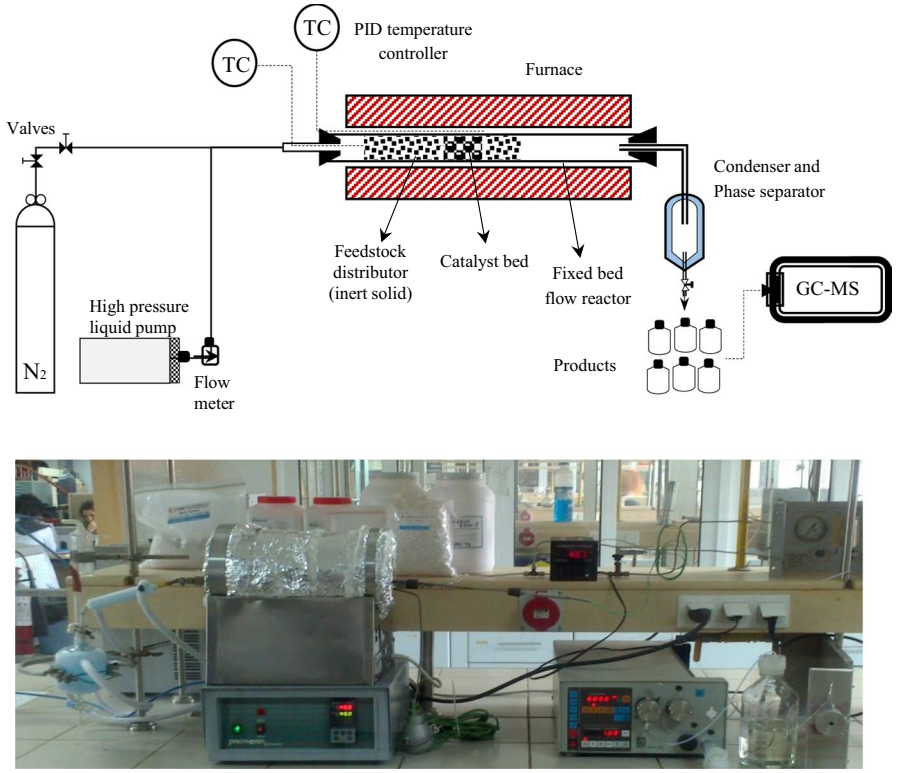

Fig. 1 Schematic representation and picture of the experimental setup

on stream (TOS) during the reaction, which ranged from 0.5 to 6 h. The products were then analysed using a Thermo-Finnegan gas chromatograph with a mass spectrometer detector (Zebron column, ZB-1MS, 60 m×0.25 mm). The same oven temperature programme was used in the analysis as mentioned previously.

Conversions of naphthalene was determined using Eq. (1) [24]. Distribution of naphthalene, methylnaphthalenes (MNs), and dimethylnaphthalenes (DMNs) were determined based on the naphthalene compounds in the products as shown in Eq. (2)–(4). Distribution of each methylnaphthalene compounds and DMN-triads were defined in total MNs and DMNs as presented in Eq. (5) and (6) [26]. The selectivity of 2,6-DMN and 2,7-DMN were defined the ratio in the DMNs [Eq. (7), (8)]. The ratio of 2,6-DMN to 2,7-DMN was also determined using Eq. (9).

$$\text{Conversion of Naphthalene (wt\%)} = \frac{m_{\text{Naph},0} - m_{\text{Naph},t}}{m_{\text{Naph},0}} * 100 \tag{1}$$

$$\text{Naph distributions (wt\%)} = \frac{m_{\text{Naph}}}{m_{\text{Naph}} + m_{\text{MNs}} + m_{\text{DMNs}}} * 100 \tag{2}$$

$$\text{MN distributions (wt\%)} = \frac{m_{\text{MNs}}}{m_{\text{Naph}} + m_{\text{MNs}} + m_{\text{DMNs}}} * 100 \tag{3}$$

$$\text{DMN distributions (wt\%)} = \frac{m_{\text{DMNs}}}{m_{\text{Naph}} + m_{\text{MNs}} + m_{\text{DMNs}}} * 100 \tag{4}$$

$$\text{MN} - \text{molecules distribution (wt\%)} = \frac{m_{i-\text{MN}}}{m_{\text{MNs}}} * 100 \tag{5}$$

$$\text{DMN} - \text{triad distribution (wt\%)} = \frac{m_{j-\text{triad}}}{m_{\text{DMNs}}} * 100 \tag{6}$$

$$2,6 - \text{DMN selectivity} = \frac{m_{2,6-\text{DMN}}}{m_{\text{DMNs}}} * 100 \tag{7}$$

$$2,7 - \text{DMN selectivity} = \frac{m_{2,7-\text{DMN}}}{m_{\text{DMNs}}} * 100 \tag{8}$$

$$2,6/2,7\,\text{ratio} = \frac{m_{2,6-\text{DMN}}}{m_{2,7-\text{DMN}}} \tag{9}$$

where $m_{\text{Naph},0}$ and $m_{\text{Naph},t}$ are the weight of naphthalene in the feed and products, respectively. m_{Naph}, m_{MNs} and m_{DMNs} represent the total mass percentages of naphthalene, MNs, and DMNs, respectively, at the time on stream of t. $m_{i\text{-MN}}$ represents the total mass percentages of 1-MN or 2-MN in the product stream at the time on stream of t. $m_{j\text{-triad}}$ represents the total mass percentages of DMN-triads (2,6-triad: 1,5-DMN + 1,6-DMN + 2,6-DMN, 2,7-triad: 1,8-DMN + 1,7-DMN + 2,7-DMN, 2,3-triad: 1,4-DMN + 1,3-DMN + 2,3-DMN) at the time on stream of t. $m_{2,6\text{-DMN}}$ and $m_{2,7\text{-DMN}}$ demonstrate the mass percentage of 2,6-DMN and 2,7-DMN, respectively, at the time on stream of t.

Coke formation

After catalysts have been used, they have accumulated coke on their surfaces. Following the testing procedures, the used catalysts were removed from the tubular reactor and subjected to the process of determining the amount of coke. For the determination of the coke deposited on catalyst, the used catalyst was placed in a porcelain crucible and dried at 120 °C for 9 h to remove moisture and volatile substances other than coke. The coke on the dried catalysts were then combusted at 450 °C for an hour and 650 °C for 4 h. The weight loss due to the coke combustion determined using Equation (10).

$$\%\text{Coke (wt\%)} = \frac{m_{\text{DryCokeCat}} - m_{\text{CleanCat}}}{m_{\text{DryCokeCat}}} \quad (10)$$

where $m_{\text{DryCokeCat}}$ and m_{CleanCat} represent the mass of the coke deposited catalyst after dying process and the mass of the cleaned catalyst after the combustion process.

Results and discussion

Catalyst characterisation

Nitrogen sorption isotherm of HBeta is given in Fig. 2a. The sorption isotherm of HBeta is corresponding to Type IV which is typical of mesoporous materials according to IUPAC classification. The isotherm shows a wide hysteresis cycle starts at the relative pressure of 0.4 which also suggest the presence of the mesoporous material. The BET surface area and BJH pore volume of HBeta was determined as 432 m^2/g and 0.345 cm^3/g. The acidity of the HBeta was measured using the absorbance along with Pyridine-IR spectra, presented in Fig. 2b. The acidity of the zeolite catalysts defined by the absorbance values at 1450 cm^{-1} for Lewis about 1495 cm^{-1} for Lewis and Bronsted and about 1550 cm^{-1} for Bronsted acid sites. The ratio of Lewis to Bronsted was determined as 1.12 using the acidity levels at 1450 cm^{-1} and 1550 cm^{-1}, these findings correlate with those by Niftaliyeva et al. [7] and Jin et al. [29].

The energy-dispersive X-ray (EDX) mapping and scanning electron microscope (SEM) images (Fig. 3a, b) were carried out to provide information about chemical composition, crystalline structure, the external morphology (texture) on the surface of the HBeta catalyst. The HBeta zeolite catalyst has an irregular external shape having coarse external surfaces as shown in Fig. 3a. Additionally, the catalyst demonstrates a homogeneous distribution of aluminium and silicon on the surface of the particles.

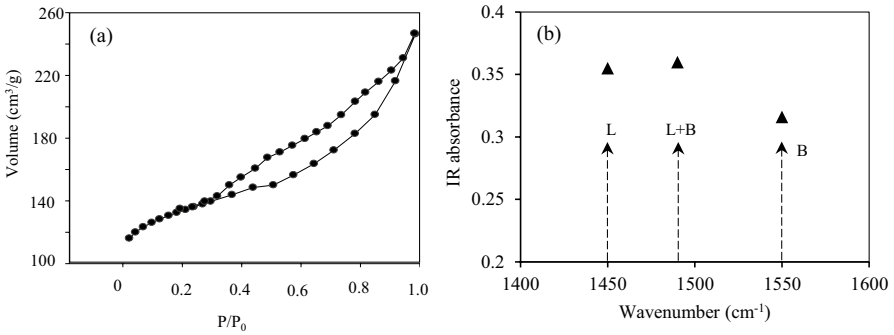

Fig. 2 **a** Nitrogen sorption isotherm (obtained at 77 K) and **b** Pyridine-IR spectra of HBeta

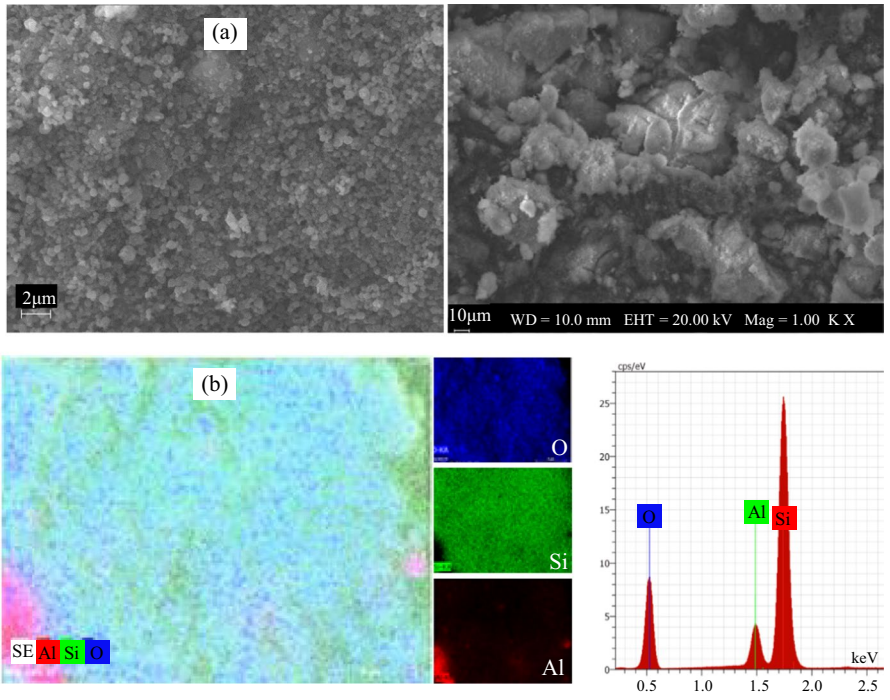

Fig. 3 **a** SEM image and **b** EDX mapping of HBeta zeolite catalyst

The Fourier transform infrared (FTIR) spectrum of HBeta (presented in a previous publication [7, 49] contains a group of absorption bands such as O–H groups (about 3300–3600 cm^{-1}) [50], external asymmetric stretching of T–O–T (1212 cm^{-1}), main T–O–T vibrations (1100 cm^{-1}), internal asymmetric stretching of the T–O–T (1090 cm^{-1}), and the internal bonds of the tetrahedral SiO_4 structural (805 cm^{-1}) [24]. Furthermore, the bands at 520 and 465 cm^{-1} indicate the presence of five membered double rings, typical of Beta zeolite and assigned to vibrations of T–O–T (T: Si or Al) siloxane bonds in the ring, respectively [24, 51]. The X-ray diffraction (XRD) patterns of HBeta is presented in Fig. 4, in which the peaks at $2\theta = 7.8°$, 21.6°, 22.6°, 25.3°, 27.0°, and 29.6° represent the main crystal structure of Beta zeolite catalyst [52–54].

Composition of CTNOF and potential reaction mechanisms

Chemical composition of CTNOF

The composition of coal tar naphthalene oil fraction (CTNOF) was identified using the GC–MS and results are presented in Fig. 5. Naphthalene is the most abundant single component of CTNOF; containing about 60 wt% of naphthalene, 11.5 wt% of methylnaphthalenes (MNs) and 12.7 wt% of dimethylnaphthalenes (DMs). In

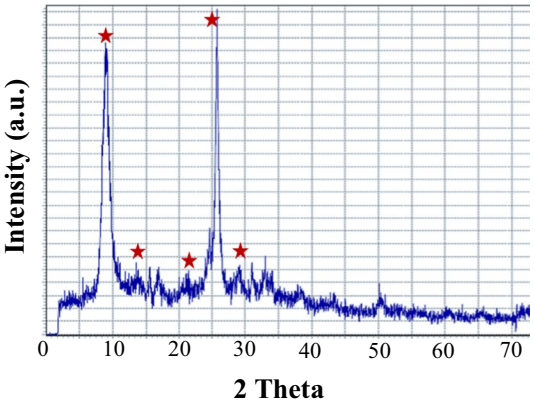

Fig. 4 XRD pattern of HBeta zeolite catalyst

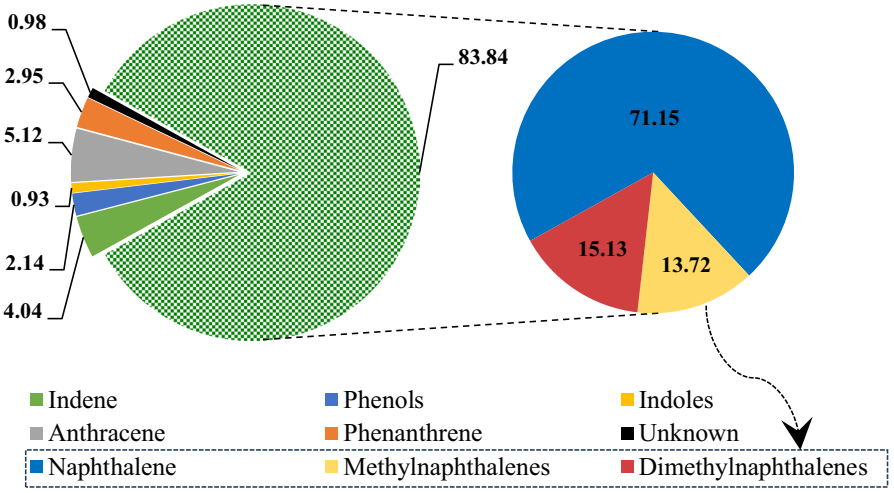

Fig. 5 Chemical compositions of coal tar naphthalene oil fraction (CTNOF)

addition to naphthalene compounds, the CTNOF contains a wide range of other value-added aromatic compounds. Indene (C_9H_8, 4.0 wt%) is used in the production of indene/coumarone thermoplastic resins. Indole (C_8H_7N, 0.9 wt%) regulates various aspects of bacterial physiology, including plasmid stability, biofilm formation, spore formation, resistance to drugs, and virulence as an intercellular signal molecule. Phenols (C_6H_5OH, 2.1 wt%) are widely used in household products as a disinfectant and in medicine as a surgical antiseptic, in industrial synthesis as intermediates such as a starting material to make plastics, explosives such as picric acid, and drugs such as aspirin. Anthracene ($C_{14}H_{10}$, 5.1 wt%) and Phenanthrene ($C_{14}H_{10}$, 2.9 wt%) are used in the production of dyes, plastics and pesticides, explosives, and drugs. These compounds make CTNOF is an important feedstocks for the production of value added chemicals. The following "Potential reaction mechanisms"

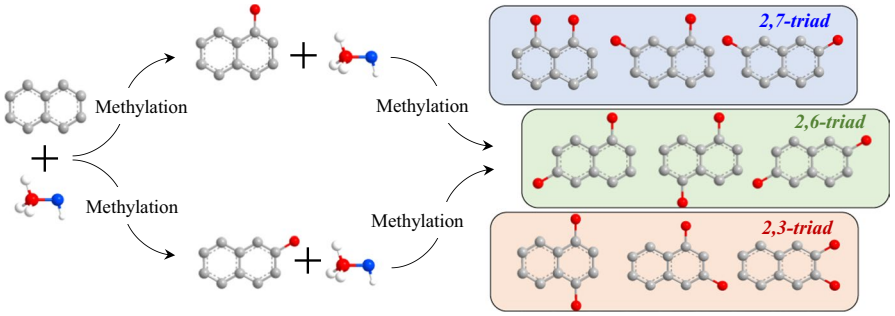

Fig. 6 Methylation of naphthalene and MNs (2-MN and 1-MN)

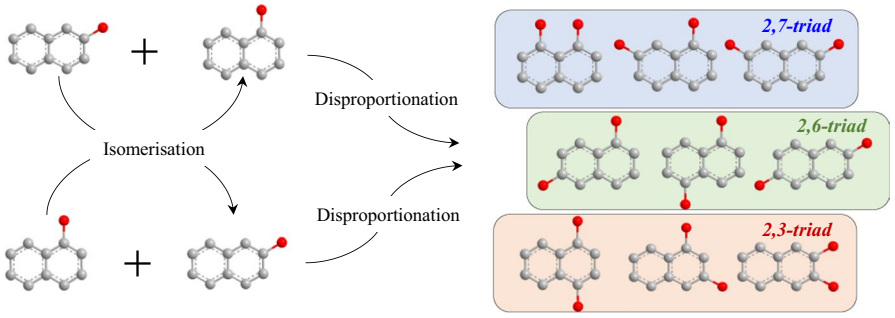

Fig. 7 Isomerisation and disproportionation of MNs (2-MN and 1-MN)

section presents the reaction mechanisms on how to produce fine value added chemicals using the naphthalene sources in CTNOF.

Potential reaction mechanisms

Methylation tests of CTNOF with methanol were carried out on HBeta in a fixed-bed reactor. The possible reaction pathways of naphthalene derivatives with methanol are demonstrated in Figs. 6, 7 and 8. Figure 6 demonstrates the potential methylation reactions and mechanisms, where the naphthalene compounds can react with methanol and produce 2-MN and 1-MN. The produced MNs can also provide a further methylation reaction to DMNs. The second reaction could be the isomerisation reaction between MN compounds (from 1-MN to 2-MN, or opposite) as demonstrated in Fig. 7. MNs compounds can also provide a disproportionation reaction to produce DMNs. In addition to methylation (Fig. 6) and disproportionation (Fig. 7) reactions paths, the produced DMNs compounds (9 different compounds) can also show isomerisation reaction with other DMN compounds (Fig. 8). Thanks to these isomerisation and isomerisation reaction, a specific type of DMN compound (i.e., 2,6-DMN) can be produced.

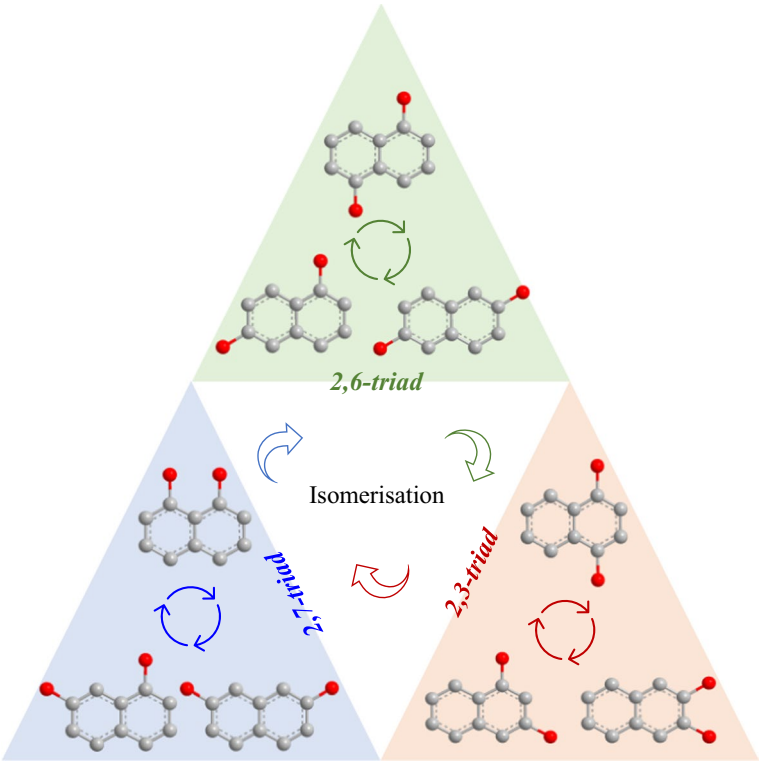

Fig. 8 Isomerisation of DMNs in groups of 2,6-triad, 2,7-triad and 2,3-triad

Methylation of CTNOF

Naphthalene conversion

The conversion of naphthalene and the distribution of naphthalene derivatives (Naphthalene, MNs, and DMNs) in product stream are presented in Fig. 9 through time on stream (continuous reaction time) over HBeta zeolite catalyst. The product selectivity of naphthalene derivatives for the methylation of CTNOF are presented in Table 2. The naphthalene conversion reached to 99 wt% for 0.5 h of time on stream. However, it is then gradually decreased with time on stream and then reached to about 10–20 wt% after 3.5–4.0 h. Figure 9b shows that significant amount of naphthalene compounds is converted to methylnaphthalenes at the early stage of the reaction. The naphthalene was predominantly converted to 2-MN (Table 2). As the naphthalene distribution drastically decreased from 74 wt% (in the CTNOF feedstock) to 2 wt%, while the methylnaphthalene distribution was jumped from 14 wt% (in CTNOF feedstock) to 87 wt% at the early stage of the reaction (0.5 h). The conversion of naphthalene is gradually decreased with time on stream which resulted in lower methylnaphthalene productions through

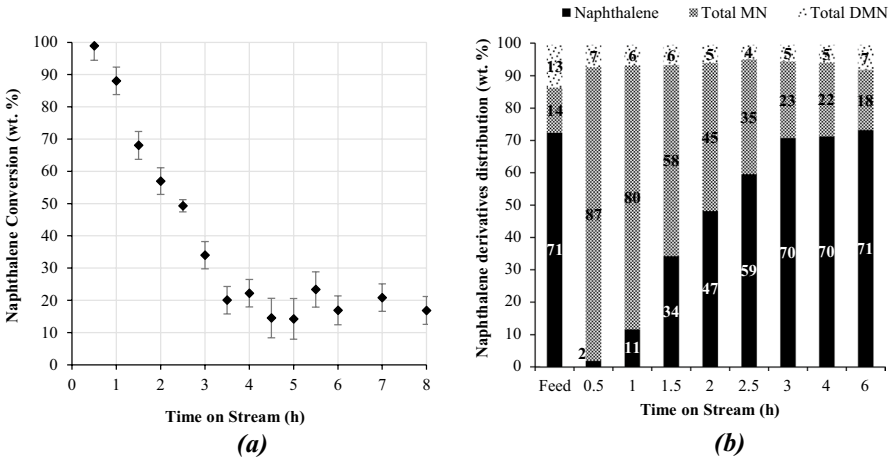

Fig. 9 **a** Naphthalene conversion and **b** distributions of naphthalene derivatives with time on stream over HBeta

Table 2 Product selectivity of naphthalene derivatives and ratio of 2,6-DMN/2,7-DMN for the methylation of CTNOF

Time on stream (h)	CTNOF	0.5	1.0	1.5	2.0	2.5	3.0	4.0	6.0
Methylnaphthalene distribution (wt%)									
2-MN	73.5	93.8	93.3	91.9	91.3	91.2	87.6	87.3	85.6
1-MN	26.5	6.2	6.7	8.1	8.7	8.8	12.4	12.7	14.4
Dimethylnaphthalene distribution (wt%)									
2,6-DMN	5.1	34.8	27.7	21.6	20.3	17.6	11.6	9.5	6.8
1,5-DMN	22.3	1.9	12.3	22.6	26.1	25.1	40.3	43.3	42.9
1,6-DMN	10.4	3.8	7.8	7.4	8.4	9.0	4.5	3.7	2.6
1,7-DMN	7.3	27.0	27.5	22.5	19.6	18.2	13.2	11.0	8.2
1,8-DMN	29.8	0.5	1.9	3.6	4.7	7.9	12.0	14.5	17.8
2,7-DMN	4.9	31.7	21.1	19.0	17.0	15.8	10.0	8.4	5.9
2,3-DMN	20.2	0.4	1.8	3.4	3.9	6.3	8.3	9.6	15.8
1,4-DMN	10.2	12.1	11.3	11.1	9.7	8.7	7.4	6.9	5.9
1,3-DMN	3.6	13.5	13.7	11.2	9.8	9.1	6.6	5.5	4.1

methylation of CTNOF. Although the DMN derivative distribution decreased from 13 wt% to ~ 5–7 wt% with time on stream (Fig. 9b), the selectivity of 2,6-DMN increased from 5 wt% in CTNOF feedstocks to 35 wt% at the early stage of time on stream (0.5 h) (Table 2).

Gradual deactivation of the HBeta zeolite catalyst due to the coke deposition is one of the main reasons for the decrease in naphthalene conversion. During the methylation, disproportionation, and isomerisation reaction, carbon tends to deposit over the catalyst surface [55]. This coke deposition can block active sites on the

catalyst, reducing its effectiveness in promoting the desired reactions [56], including naphthalene methylation. Details of coke deposition are provided in the "Coke formation and impact on methylation of CTNOF" section. In the methylation of CTNOF over the HBeta, the residence time plays a crucial role in coke deposition, especially when considering the potential for continuous operation over an extended period without regeneration. In order to understand the limitations of the HBeta zeolite catalyst, the experiment was operated under 8 h of TOS without regeneration in this study. Since the timescale of coke formation is much shorter than the timescale for conversion [57]. In industrial applications, such as fluid catalytic cracking (FCC) units in refineries, coke deposition is a common challenge encountered during heterogeneous catalytic reactions [58–61]. In conventional FCC units, continuous regeneration processes are employed to mitigate catalyst deactivation caused by coke buildup [59–62]. These regeneration units play a vital role by combusting the deposited coke, releasing energy that can be harnessed to drive the endothermic cracking reactions [58, 62]. This synergy between coke combustion and the exothermic cracking reaction is balanced and essential for maintaining catalytic activity [59].

To draw a parallel to the methylation of CTNOF, it could be conceivable that a similar approach could be applied following reaction optimisation. By integrating a regenerator into the methylation of CTNOF, coke deposition could be managed effectively, thus ensuring sustained catalytic activity over extended periods. However, it is important that the feasibility of applying such a regenerative approach to the methylation of CTNOF would depend on several factors, including the specific reaction kinetics, the rate of coke deposition, and the design of the regenerator, and most importantly the residence time of the catalyst in each reactor. As shown in this study, shorter residence times in the methylation of CTNOF will achieve high conversion and desired product distribution and minimise undesirable side reactions, such as excessive amount of coke deposition. It is, therefore, crucial to perform detailed modelling, experimentation, and optimisation to determine the optimal residence time and other operating parameters for our specific reaction system.

Table 2 shows that while there is a rise in the selectivity of 2,6-DMN, 2,7-DMN, 1,3-DMN and 1,7-DMN, a sharp decrease can be observed in the selectivity of other DMN isomers. Although the methylation of CTNOF mainly support the naphthalene conversion to 2-MN, the methylation of 2-MN to DMNs may also have taken place. The increase in 2,6-DMN can also be attributed to the isomerisation of other DMN and methylation of MNs. The selectivity of 2,6-DMN for the first hours are comparable with that found in studies [24, 26, 31, 42, 44, 45].

Methylnaphthalene distributions

Figure 10 shows the methylene naphthalene distribution through the reaction. The methylene naphthalene distributions in the feedstocks are 74 wt% for 2-MN and 26 wt% for 1-MN. The methylation of CTNOF over HBeta zeolite catalysts clearly contributed to the formation of further 2-MN as the increase in the ratio of 2-MN and decrease in the ratio of 1-MN provides that the naphthalene preferable converts to 2-MN rather than 1-MN, which is an important compound considering the

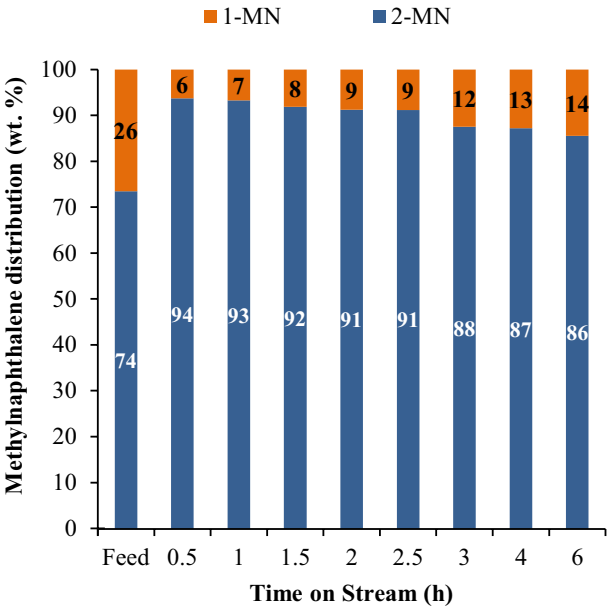

Fig. 10 Distributions of methylnaphthalenes (MNs) derivatives

application of 2-MN in the production of vitamin K and 2,6-DMN. Through the reaction, the ratio of 2-MN decrease, while the ratio of 1-MN increase in the product stream, which could be attributed to the decrease in the conversion of naphthalene to 2-MN (as shown in Fig. 5a) due to the carbon deposition in pores (catalyst poisoning). However, Fig. 10 shows that even after the conversion decrease to the lowest value at 3 h, the catalyst convert the 1-MN to 2-MN, as the ratio of 2-MN is between 86 and 88 wt% at the TOS of 3–6 h, which is still higher than the ratio of 2-MN in the feedstocks (74 wt%), which could be attributed to the isomerisation of 1-MN to 2-MN over poisoned HBeta zeolite catalysts.

Dimethylnaphthalene distributions

Figure 11 shows the distributions of dimethylnaphthalenes triads (i.e., 2,6-triad, 2,7-triad, and 2,3-triad) and individual DMNs. The distribution of 2,6-triad DMNs demonstrate an increase from 38 wt% in feedstocks to 52–55 wt% with increasing the time on stream (Fig. 11a), which could be attributed to the conversion of MNs to DMNs but also potential isomerisation reaction from other DMNs in the 2,7-triad and 2,3-triad. Unlike 2,6-triad DMNs, the distribution of 2,3-triad DMNs in the product stream decrease from 34 to 22–26 wt% through time of stream. Although there is an increase in the 2,7-triad DMNs compounds from 42 to 59–50 wt% in the early stage of reaction (0.5–1.0 h), it was then decreased back to 42 wt% at about 2–2.5 h of TOS, and then further decrease to 32 wt% at the later stage of reaction (TOS = 6.0 h).

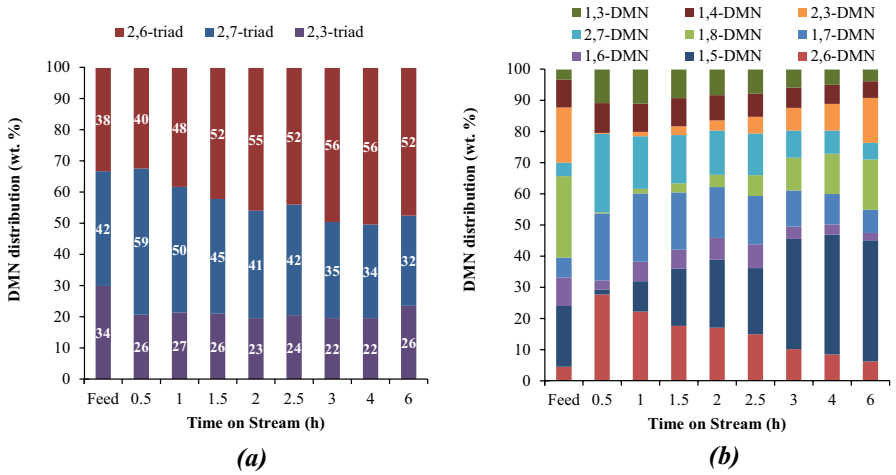

Fig. 11 Distributions of **a** DMN-triads (2,6-, 2,7-, and 1,3-triad DMNs) derivatives and **b** individual DMNs compounds

The increase in the early stage could be attributed to the high conversion of naphthalene over fresh catalyst, while the decrease at the later stage could be clarified by the isomerisation of DMNs [49] and/or degradation of DMNs to MNs. The accumulative number of each triad groups (Fig. 7a) through time on streams shows that the isomerisation is not only within the triad groups but also between the DMNs compound within different triad groups. Figure 11b demonstrates the distribution of each type of individual DMNs with time on stream. Identification of each reaction (the trend in Fig. 11b) for DMN compounds deems something impossible. As the DMN distribution could change due to several reactions, i.e., (1) through isomerisation of DMNs from one from to another, (2) methylation of MNs to DMNS, (3) two stage methylation of naphthalene. As all these three possibilities cause a wide range of pathways and predicting the reaction pathways is significantly difficult.

However, studies show that the isomerisation between DMN compounds tends within the triad groups [7] as shown in Fig. 12. The percentage distribution of each type DMNs within the triad groups are presented in Fig. 12a (for 2,6-triad DMNs), b (for 2,7-triad DMNs), and c (for 2,3-triad DMNs), while the numbers over the bars present the percentage distribution of each type of DMNs within the total DMNs products. In the 2,6-triad groups (Fig. 12a), the distribution of 1,5-DMN decrease from 22 to 2 wt%, while the distribution of 2,6-DMN increase from 5 to 35 wt% at the early stage of the reactions (0.5 h). Similar trends were observed for 2,7-triad groups (Fig. 12b), where the distribution of 1,8-DMN decrease from 30 to 0 wt% while the distribution of 2,7-DMN and 1,7-DMN increase from 5 to 30 wt% and 7–27 wt%, respectively. Furthermore, similar trends were observed within the

2,3-triad groups (Fig. 12c) in which 2,3-DMN decrease, while 1,3-DMN increase at the early stage of time on stream (0.5 h). However, this trend tends to revers through the time on streams for each type of DMN compounds, which could be attributed to the catalyst poisoning and losing catalytic activity.

2,6- and 2,7- dimethylnaphthalenes

Figure 13 shows the selectivity of 2,6-DMN and 2,7-DMN in addition to the ratio of 2,6- to 2,7-DMNs. As one of the most significant value-added products in DMN compounds, 2,6-DMN is a crucial starting molecule for the synthesis of high-performance polyester resins such as polyethylene naphthalate (PEN) and polybutylene naphthalate (PBN). Higher selectivity of 2,6-DMN would be one of the most desirable step in the utilisation of CTNOF. Figure 13 shows that at the early stage of the reaction, the selectivity of 2,6-DMN jumped to 35 wt% and then it shows gradual decrease through time on streams and reached to the starting point ~ 5 wt% after 6 h of time on stream. Similar trend was observed for the selectivity of 2,7-DMN, which is a side product demonstrating very similar characteristics as 2,6-DMN. The ratio of 2,6- to 2,7-DMNs were observed to increase about 1.4 at the early stage and then decreased and stabilised at around ~ 1.1, which provides at any time on stream the selectivity of 2,6-DMN is higher than the selectivity of 2,7-DMN.

Initially, at the early stage of the methylation reaction over HBeta, there is a dynamic change in the distribution of intermediates and products, which could be attributed to variations in the rates of individual methylation reactions and isomerisation processes over the fresh HBeta zeolite catalyst. During this period, the position of "2" in naphthalene could be more reactive as the synthesis of 2-MN significantly increase. Furthermore, the position of "6" in 2-MN could be more reactive than "7", which propose the formation of 2,6-DMN is more favoured than that 2,7-DMN, which also demonstrated for another zeolite catalyst; ZSM-5 [63]. Over the time on stream, the coke deposited external surface and then internal surface of HBeta, which potentially caused a significant decrease in the conversion of naphthalene and selectivity of 2,6-DMN and 2,7-DMN. Since the internal coke proved to be much more detrimental than the external coke [64]. Calculation results indicated that 2,7-DMN is slightly smaller than 2,6-DMN in molecular dimension, which can easily explain the unusual 2,6-DMN/2,7-DMN ratio observed in experiment, that is, the 2,6-DMN/2,7-DMN ratio decreases when the pore of HBeta is narrowed due to coke deposition, which is very similar for the ZSM-5 [63]

Given their closely matched molecular dimensions of 2,6-DMN and 2,7-DMN, these isomers share similar kinetic characteristics during the methylation process. Consequently, changes in reaction conditions or catalyst activity can affect the production of 2,6-DMN and 2,7-DMN nearly simultaneously. This phenomenon

Fig. 12 Distributions of **a** 2,6-triads **b**, 2,7-triads and **c** 2,3-triads derivatives. "y" axis provides the distribution of triads and the numbers on the bars represents the percentage distribution of each DMNs in the total DMN mixture (an extended version of Fig. 7b) ▶

is in line with the principles of chemical kinetics, where molecules of similar size and structure often exhibit analogous reactivity patterns. As a result, even subtle alterations in the reaction environment or catalyst behaviour can lead to concurrent increases or decreases in the selectivity of both isomers, contributing to the observed stabilisation of their ratio over time.

Coke formation and impact on methylation of CTNOF

A significant coke deposition of 22 wt% over the HBeta catalyst during the methylation and disproportionation of CTNOF was observed. Coke deposition refers to the buildup of carbonaceous material on the catalyst surface, which have negatively impact on catalyst performance and activity over time. Such a high level of coke deposition could have several implications:

- *Catalyst Activity* coke deposition can block active sites on the catalyst surface, leading to reduced catalytic activity. As coke accumulates, it can hinder the reactants' access to the catalyst's active sites, leading to lower reaction rates. This is potentially the reason for a significant decrease in the naphthalene conversion demonstrated in Fig. 9.
- *Selectivity* the presence of coke can alter the selectivity of the catalyst, causing a shift in the product distribution of the reaction. This can result in changes to the desired and undesired products. As demonstrated in Fig. 10, the 2-MN distribution decreased, while the 1-MN distribution increased with time on stream. Similarly, Fig. 11b and Fig. 12a show a significant decrease in 2,6-DMN distribution with time on stream.
- *Catalyst deactivation* over time, excessive coke deposition can lead to catalyst deactivation, meaning the catalyst becomes less effective at promoting the desired reaction, which could be observed in Fig. 9a, the catalyst shows significantly low activity after 3.5 h of run.

To mitigate the negative effects of coke deposition, it's essential to implement proper catalyst regeneration or replacement strategies. Additionally, optimising reaction conditions, such as temperature, flow rate, residence time, and reaction times, can help reduce coke formation in the methylation of CTNOF. Furthermore, a process design, i.e., fluid catalytic cracking, could be a potential process configuration where the coke deposition can be regenerated in a fluidised bed reactor and the produced energy can be used in the methylation reaction.

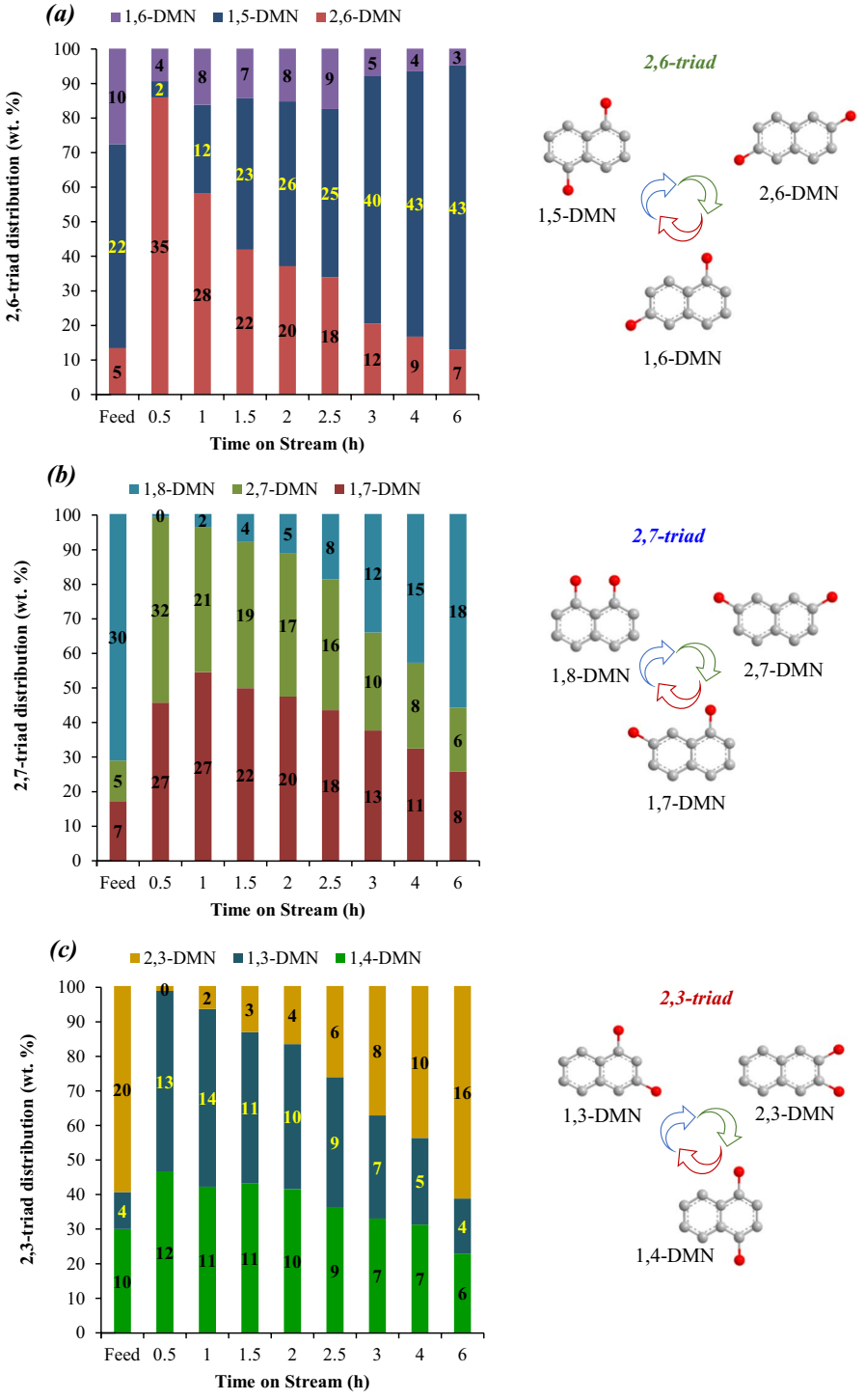
(a)
1,6-DMN
1,5-DMN
2,6-DMN
2,6-triad
1,5-DMN
2,6-DMN
1,6-DMN
2,6-triad distribution (wt. %)
Time on Stream (h)
Feed 0.5 1 1.5 2 2.5 3 4 6
(b)
1,8-DMN
2,7-DMN
1,7-DMN
2,7-triad
1,8-DMN
2,7-DMN
1,7-DMN
2,7-triad distribution (wt. %)
Time on Stream (h)
Feed 0.5 1 1.5 2 2.5 3 4 6
(c)
2,3-DMN
1,3-DMN
1,4-DMN
2,3-triad
1,3-DMN
2,3-DMN
1,4-DMN
2,3-triad distribution (wt. %)
Time on Stream (h)
Feed 0.5 1 1.5 2 2.5 3 4 6

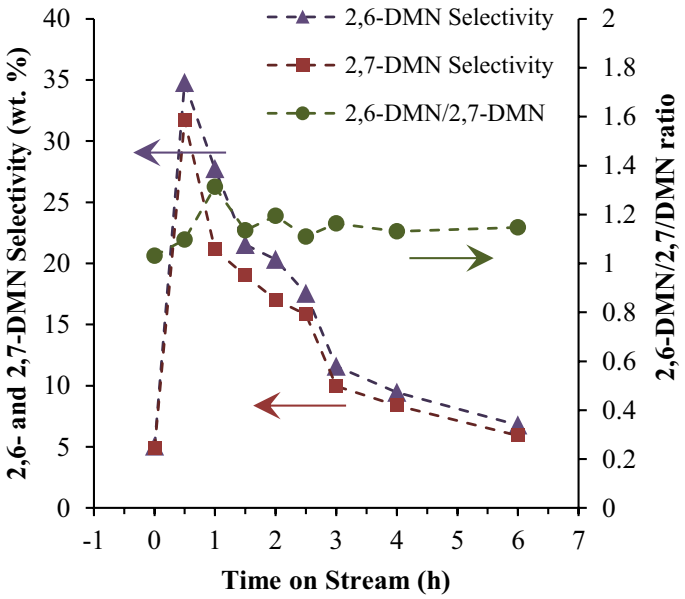

Fig. 13 Selectivity of 2,6-DMN and 2,7-DMN and the ratio of 2,6-/2,7-DMN

Conclusions

The novelty of this paper is to investigate the methylation and isomerisation of a non-valuable industrial waste material; CTNOF, on HBeta zeolite catalyst to the synthesis of value-added chemicals such as 2-MN and 2,6-DMN. The GC–MS analysis of CTNOF demonstrated that the waste mixture consists of approximately 83.8 wt% of naphthalene compounds; 71.5% of naphthalene, 13.72 wt% of methylnaphthalenes, 15.13 wt% of dimethylnaphthalenes. With methylation reactions, the percentage of naphthalene dramatically decrease from 71.5 wt% to about ~ 2 wt% at the early stage of the methylation reaction (30 min), whereas the percentage of 2-MN sharply increased from 10 to 82 wt%. While naphthalene conversion initially reaches 99 wt% within 0.5 h of operation, it gradually decreases to approximately 10 wt% over extended run times. Notably, coke deposition significantly deactivates the HBeta zeolite catalyst during CTNOF methylation, impacting naphthalene conversion. At the early stage of the reactions, the selectivity of 2,6-DMN reached to 35 wt%. This study has demonstrated that CTNOF is an alternative feedstock for the direct synthesis of value-added chemicals; 2,6-DMN and 2-MN, via methylation over HBeta zeolite catalysts. As future work, the feedstock (CTNOF) could be effectively used for the synthesis of value-added chemicals over composite zeolite catalysts i.e. ZSM-5/Beta to promote isomerisation reaction in addition to methylation and disproportionation. Adding noble metals could also enhance the activity and maximise the selectivity of 2,6-DMN. Furthermore, the study will be extended to a comprehensive understanding the effects of process conditions; reaction

temperature, space velocity, pressure, and reactant ratios on the conversion efficiency of CTNOF and the production of target products.

Supplementary Information The online version contains supplementary material available at https://doi.org/10.1007/s11164-023-05158-5.

Acknowledgements The authors gratefully acknowledge the generous support and funding provided by The Scientific and Technological Research Council of Turkey (TÜBİTAK, Project No: 112M297) and Ankara University Scientific Research Projects Department (Project No: 15B0443009). We extend our sincere appreciation to Prof. Dr. Zeki Aktaş for his invaluable support and expertise in surface analysis, which greatly contributed to the success of this project.

Authors' contribution FG contributed to conceptualisation, formal analysis, investigation, validation, visualisation, project administration, funding acquisition, writing—original draft, and writing—review and editing. AOK done investigation, AK contributed to conceptualisation, supervision, project administration, and funding acquisition.

Funding This work was supported by the Scientific and Technological Research Council of Turkey [TÜBİTAK, Project No: 112M297]; and Ankara University Scientific Research Projects Department [Project No: 15B0443009].

Availability of data and materials All relevant data are within the manuscript and available from the corresponding author upon request.

Declarations

Conflict of interest The authors declare that they have no competing interests.

Ethical approval Not applicable.

Open Access This article is licensed under a Creative Commons Attribution 4.0 International License, which permits use, sharing, adaptation, distribution and reproduction in any medium or format, as long as you give appropriate credit to the original author(s) and the source, provide a link to the Creative Commons licence, and indicate if changes were made. The images or other third party material in this article are included in the article's Creative Commons licence, unless indicated otherwise in a credit line to the material. If material is not included in the article's Creative Commons licence and your intended use is not permitted by statutory regulation or exceeds the permitted use, you will need to obtain permission directly from the copyright holder. To view a copy of this licence, visit http://creativecommons.org/licenses/by/4.0/.

References

1. D. Wang, L. Jin, Y. Li, B. Wei, D. Yao, T. Wang, H. Hu, Fuel Process. Technol. **191**, 20 (2019)
2. L. Han, R. Zhang, J. Bi, Fuel Process. Technol. **90**, 292 (2009)
3. D. Zhang, P. Liu, X. Lu, L. Wang, T. Pan, Fuel Process. Technol. **141**, 117 (2016)
4. Z.-H. Ma, X.-Y. Wei, G.-H. Liu, F.-J. Liu, Z.-M. Zong, Fuel **292**, 119954 (2021)
5. C. Li, K. Suzuki, Resour. Conserv. Recycl. **54**, 905 (2010)
6. C. Song, H.H. Schobert, Fuel Process. Technol. **34**, 157 (1993)
7. A. Niftaliyeva, F. Güleç, A. Karaduman, Res. Chem. Intermed. **46**, 2403 (2020)
8. F. Güleç, A. Özen, A. Niftaliyeva, A. Aydın, E.H. Şimşek, A. Karaduman, Res. Chem. Intermed. **44**, 55 (2018)

9. F. Güleç, A. Niftaliyeva, A. Karaduman, Res. Chem. Intermed. **44**, 7205 (2018)
10. I.D.G.A. Putrawan, T.H. Soerawidjaja, Sep. Purif. Technol. **39**, 79 (2004)
11. J.X. Zhang, Adv. Mater. Res. **619**, 286 (2013)
12. E. Gabano, E. Perin, D. Bonzani, M. Ravera, Inorg. Chim. Acta **488**, 195 (2019)
13. X. Tian, J. Zhang, F. Zhang, M. Zhao, Z. Chen, K. Zhou, P. Zhang, X. Ren, X. Jiang, X. Mei, Colloids Surf. B Biointerfaces **165**, 278 (2018)
14. M. Takagawa and R. Shigematsu, Process for producing highly pure 2,6-dimethylnaphthalene (Google Patents, 2000)
15. E.H. Şimşek, F. Güleç, H. Kavuştu, Fuel **207**, 814 (2017)
16. G. Azpíroz, C.G. Blanco, C. Banciella, Fuel Process. Technol. **89**, 111 (2008)
17. H.-S. Xu, J.-H. Zhao, C.-Y. Song, L.-C. Wang, R.-J. Bai, Chem. React. Eng. Technol. **18**, 334 (2002)
18. M. Florea, R. Marin, F. Pălăşanu, F. Neaţu, V. Pârvulescu, Catal. Today **254**, 29 (2015)
19. T. Komatsu, Y. Araki, S. Namba, T. Yashima, Stud. Surf. Sci. Catal. **84**, 1821 (1994)
20. R. Millini, F. Frigerio, G. Bellussi, G. Pazzuconi, C. Perego, P. Pollesel, U. Romano, J. Catal. **217**, 298 (2003)
21. C. Zhang, X.W. Guo, Y.N. Wang, X.S. Wang, C.S. Song, Chin. Chem. Lett. **18**, 1281 (2007)
22. L. Jin, X. Zhou, H. Hu, B. Ma, Catal. Commun. **10**, 336 (2008)
23. J. Van der Mynsbrugge, M. Visur, U. Olsbye, P. Beato, M. Bjørgen, V. Van Speybroeck, S. Svelle, J. Catal. **292**, 201 (2012)
24. F. Güleç, E.H. Şimşek, A. Karaduman, J. Fac. Eng. Archit. Gazi Univ. **31**, 609 (2016)
25. S.-B. Pu, T. Inui, Appl. Catal. A Gen. **146**, 305 (1996)
26. M. Motoyuki, K. Yamamoto, S. Yoshida, S. Yamamoto, A.V. Sapre, J.P. Mc Williams, S.P. Donnelly and S.D. Hellring, Isomerization of dimethylnaphthalene to produce 2, 6-dimethylnaphthalene (Google Patents, 2000)
27. R. Brzozowski, W. Skupiński, J. Catal. **220**, 13 (2003)
28. T. Tsutsui, K. Ijichi, T. Inomata, T. Kojima, K. Sato, Chem. Eng. Sci. **59**, 3993 (2004)
29. L. Jin, Y. Fang, H. Hu, Catal. Commun. **7**, 255 (2006)
30. C. Song, J.-P. Shen, K.M. Reddy, L. Sun, L.D. Lillwitz, Stud. Surf. Sci. Catal. **170**, 1275 (2007)
31. X. Bai, K. Sun, W. Wu, P. Yan, J. Yang, J. Mol. Catal. A: Chem. **314**, 81 (2009)
32. L. Jin, S. Liu, T. Xie, Y. Wang, X. Guo, H. Hu, React. Kinet. Mech. Catal. **113**, 575 (2014)
33. J.-N. Park, J. Wang, C.W. Lee, S.-E. Park, Bull. Korean Chem. Soc. **23**, 1011 (2002)
34. I.-M. Tseng, J.-F. Wu, Y.-W. Chen, React. Kinet. Catal. Lett. **63**, 359 (1998)
35. G. Tasi, I. Pálinkó, F. Mizukami, React. Kinet. Catal. Lett. **74**, 317 (2001)
36. C. Dimitrov, Z. Popova, M. Tuyên, React. Kinet. Catal. Lett. **8**, 101 (1978)
37. I. Ferino, R. Monaci, L. Pedditzi, E. Rombi, V. Solinas, React. Kinet. Catal. Lett. **58**, 307 (1996)
38. W. Tang, M. Fang, H. Wang, P. Yu, Q. Wang, Z. Luo. Chem. Eng. J. **236**, 529 (2014)
39. G. Azpíroz, C. G. Blanco, C. Banciella. Fuel Process. Technol. **89**(2), 111 (2008)
40. T. Jiao, C. Li, X. Zhuang, S. Cao, H. Chen, S. Zhang. Chem. Eng. J. **266**, 148 (2015)
41. Y. H. Ding, C. H. E. N. Hang, D. F. Wang, J. F. Wang, D. P. Xu, Y. G. Wang. J. Fuel Chem. Technol. **38**(2), 140 (2010)
42. W. Wu, W. Wu, O. Kikhtyanin, L. Li, A. Toktarev, A. Ayupov, J. Khabibulin, G. Echevsky, J. Huang, Appl. Catal. A: Gen. **375**, 279 (2010)
43. Z. Liang, G. Xinwen, L. Min, W. Xiangsheng, S. Chunshan, Chin. J. Chem. Eng. **18**, 742 (2010)
44. A. Niftaliyeva, A. Karaduman, Anadolu Univ. J. Sci. Technol. A Appl. Sci. Eng. **16**, 275 (2015)
45. A. Niftaliyeva, F. Gulec, E. Simsek, M. Gullu, A. Karaduman, Anadolu Univ. J. Sci. Technol. A Appl. Sci. Eng. **16**, 167 (2015)
46. Z.-B. Wang, A. Kamo, T. Yoneda, T. Komatsu, T. Yashima, Appl. Catal. A Gen. **159**, 119 (1997)
47. T. Yashima, Z.-B. Wang, A. Kamo, T. Yoneda, T. Komatsu, Catal. Today **29**, 279 (1996)
48. V. Bogdan, A. Koklin, V. Kazanskii, Kinet. Catal. **51**, 736 (2010)
49. F. Güleç, F. Sher, A. Karaduman, Pet. Sci. **16**, 161 (2019)
50. A. Omegna, M. Vasic, J.A. van Bokhoven, G. Pirngruber, R. Prins, Phys. Chem. Chem. Phys. **6**, 447 (2004)
51. T. Saulo, A. Ernesto, R. Patrício, O. Marcelo, R. Maria do Carmo, J. Braz. Chem. Soc. **25**, 2444 (2014)
52. B. Xie, J. Song, L. Ren, Y. Ji, J. Li, F.-S. Xiao, Chem. Mater. **20**, 4533 (2008)
53. I. Sreedhar, K.S.K. Reddy, K. Raghavan, Kinet. Catal. **50**, 131 (2009)
54. A. Toktarev, L. Malysheva, E. Paukshtis, Kinet. Catal. **51**, 318 (2010)
55. M. Ahmed, Fuel Process. Technol. **92**, 1121 (2011)

56. F. Güleç, W. Meredith, C.E. Snape, J. Energy Inst. **107**, 101187 (2023)
57. M. Den Hollander, M. Makkee, J. Moulijn, Catal. Today **46**, 27 (1998)
58. F. Güleç, A. Erdogan, P.T. Clough, E. Lester, Fuel Process. Technol. **223**, 106998 (2021)
59. F. Güleç, PhD Thesis: Demonstrating the applicability of chemical looping combustion for fluid catalytic cracking unit as a novel CO_2 capture technology" in Chemical Engineering (University of Nottingham, 2020)
60. F. Güleç, W. Meredith, C.-G. Sun, C.E. Snape, Fuel **244**, 140 (2019)
61. F. Güleç, W. Meredith, C.-G. Sun, C.E. Snape, Energy **173**, 658 (2019)
62. F. Güleç, W. Meredith, C.-G. Sun, C.E. Snape, Chem. Eng. J. **389**, 124492 (2020)
63. Y. Fang, H. Hu, Catal. Commun. **7**, 264 (2006)
64. S. Lee, M. Choi, J. Catal. **375**, 183 (2019)

Publisher's Note Springer Nature remains neutral with regard to jurisdictional claims in published maps and institutional affiliations.

Authors and Affiliations

Fatih Güleç[1,2] · Aysun Koçkan[3] · Ali Karaduman[3]

✉ Fatih Güleç
Fatih.Gulec1@nottingham.ac.uk; Gulec.Fatih@outlook.com

[1] Low Carbon Energy and Resources Technologies Research Group, Faculty of Engineering, University of Nottingham, Nottingham NG7 2TU, UK

[2] Advanced Materials Research Group, Faculty of Engineering, University of Nottingham, Nottingham NG7 2RD, UK

[3] Department of Chemical Engineering, Faculty of Engineering, Ankara University, 06100 Ankara, Turkey